FERMILAB-PUB-76-108-E

LBL-4831 and
CALT-68-549
ERDA RESEARCH
AND DEVELOPMENT
REPORT

The Reaction $\pi^- p \to \eta n$ at High Energies*

O. I. DAHL, R. A. JOHNSON, R. W. KENNEY AND M. PRIPSTEIN

Lawrence Berkeley Laboratory, Berkeley, California, 94720

and

A. V. BARNES, D. J. MELLEMA, A. V. TOLLESTRUP, AND R. L. WALKER

California Institute of Technology, Pasadena, California, 91125

ABSTRACT

Measurements on the reaction $\pi^- p \to \eta n$ have been carried out at Fermilab with beam energies from 20 to 200 GeV in the same experiment in which pion charge exchange scattering was studied. The differential cross sections have a pronounced dip in the forward direction. The data can be described well by a simple Regge pole model but the resulting A_2 trajectory is not degenerate with the ρ trajectory extracted from the charge exchange data.

*Work supported in part by the U.S. Energy Research and Development Administration. Prepared under Contract E(11-1)-68 at Caltech and Contract W-7405-ENG-48 at LBL.

Submitted to Physical Review Letters - April, 1976.

The reaction $\pi^- p \to \eta n$ is a companion to pion charge exchange scattering, both theoretically and experimentally. From the theoretical point of view, these reactions are believed to be exceptionally simple so that they play a special role in the study of strong interaction dynamics, as discussed in the preceding Letter[1]. Experimentally, if one observes the η's via their 2γ decays, the two reactions differ only in the 2γ mass so that they can be easily studied in the same experiment. This has been done in previous work on this subject[2,3,4].

The experiment is simple in principle; one requires a γ-ray detector capable of identifying π^0's and η's and measuring their angle of emission, and an efficient means of eliminating background from other reactions such as $\pi^- p \to \pi^0 N^*$, $N^* \to \pi^0 n$. These basic needs impose severe requirements which must be met in the design of the apparatus. At 100 GeV, for example, the charge exchange cross section is 10^{-4} times the total cross section for all $\pi^- p$ interactions and 10^{-1} times the cross section for producing all-neutral final states. The cross section for the η reaction followed by $\eta \to 2\gamma$ decay is another factor 10 smaller.

The experimental arrangement is shown schematically in Fig. 1. Pions in the incoming beam are tagged by a threshold Cerenkov counter and their path is measured by scintillation counter hodoscopes, one near the target and the other approximately 60 m upstream[5]. The liquid hydrogen target (length 20, 40, or 60 cm) is surrounded, except for a beam entrance hole, by scintillation counters which veto all events with one or more charged particle in the final state. Outside these charged veto counters is a "Veto House" designed to be very efficient for γ-rays from $N^* \to \pi^0 n$ and other background reactions but insensitive to recoil neutrons from the charge exchange and η reactions. The Veto House counters are made of Pilot 425 Cerenkov plastic sandwiched with lead sheets. Additional lead-scintillator shower counters, V_1, V_2, V_3, V_4, cover the

remaining solid angle except for that subtended by the detector.

The detector (Fig. 1b) is a hodoscope shower detector developed for this experiment[6]. Photons from π^o, η, or other particle decays produce showers in a set of 19 parallel lead plates normal to the direction of the beam, each plate being 1.12 radiation length in thickness and 75 cm square. Gaps between the lead plates are filled (except for the two end gaps) with scintillation plastic rods 1.05 cm wide, oriented vertically and horizontally in alternate gaps. Eight scintillation rods with the same x or y coordinate (z is along the beam direction; y is up) are connected optically by curved light pipes at one end and form one counter. A number of special tricks have been employed in the construction of these counters in order to achieve a pulse height uniformity over their full length of approximately ±3%. There are 70 x-counters and 70 y-counters, whose pulse heights give the x and y distributions of the energy deposited by all photons hitting the detector.

The moments of these energy distributions may be used to obtain the combined energy (E), weighted mean position (x,y), and invariant mass (m) of the detected photons[7]. Typical uncertainties in the determination of these quantities are $\sigma_E \approx 4\%$, $\sigma_x \approx 1$ mm for π^o, and $\sigma_m \approx 7\%$ for π^o, 4.5% for η. A mass histogram showing π^o and η peaks for the 64.4 GeV data of the present experiment is illustrated in Fig. 2.

In taking data we selected neutral final state events using a relatively unrestrictive event trigger, recording pulse heights from nearly all counters on magnetic tape so that event selection criteria could be studied and adjusted later in the off-line analysis. For example, none of the gamma-ray veto counters were used in the trigger logic so that pulse height data from these counters for all neutral final state events are available for use in investigating their behavior.

Many "cuts" and corrections have been applied to the data. Fortunately it has been possible to study most of these by using the data collected in the experiment and considerable effort has been devoted to this investigation.

The results of our measurements for the reaction $\pi^- p \to \eta n$ ($\eta \to 2\gamma$) at energies 20 to 200 GeV are presented in Table 1. The differential cross sections at three of the six energies studied are also shown in Fig. 3. These data have been corrected for the effects of instrumental t-resolution and finite t bins by the procedure described in the preceding Letter on charge exchange scattering[1].

According to Regge ideas, the A_2 Regge pole is expected to dominate the η reaction so that an analysis of these data should give information about the A_2 trajectory. As in the case of pion charge exchange, our data on $\pi^- p \to \eta n$ can be described remarkably well by the simplest Regge pole model with a power law energy dependence and a nearly linear trajectory, $\alpha(t)$.

A good phenomenological description of our data is provided by the following parameterization[1]:

$$\frac{d\sigma}{dt}(s,t) = \beta(t)\, \nu^{2\alpha(t)-2} \qquad (1)$$

with $\alpha(t) = \alpha_0 + \alpha_1 t + \alpha_2 t^2$, $\beta(t) = (C_1 + C_2 t)\, e^{bt}$ and $\nu = (s - u)/4M$. The following values for the parameters have been found by a fit:

$$\alpha_0 = .371 \pm .008 \;; \quad \alpha_1 = .79 \pm .04 \;; \quad \alpha_2 = .03 \pm .04$$

$$C_1 = 306 \pm 27 \;; \quad C_2 = -9800 \pm 800 \;; \quad b = 3.80 \pm .31$$

The units are such that t is in GeV^2, ν in GeV, and $\frac{d\sigma}{dt}$ in $\mu b/GeV^2$. This fit gives a $\chi^2 = 109$ for 108 degrees of freedom. Curves calculated from the above expression are shown in Fig. 3 including an extrapolation to 5.9 GeV for comparison with the lower energy data[2]. The above parameterization, obtained by fitting our data alone, agrees only qualitatively with the lower energy data.

The trajectory $\alpha(t)$ obtained from the fit is shown by the solid curve in Fig. 4, along with "data points," $\alpha^*(t)$, obtained in the conventional manner by fitting the data at each value of t separately, using the form (1). According to the idea of "exchange degeneracy," the A_2 and ρ trajectories should be the same. Our results show that they are not, in agreement with a conclusion already reached from the previous experiments. In comparison with the ρ trajectory obtained from the charge exchange data, the A_2 trajectory found above has a smaller intercept α_0 and a smaller slope α_1 at t=0.

References and Footnotes

1. A. V. Barnes et al., preceding Letter [Phys. Rev. Lett. , (1976)].
2. O. Guisan et al., Physics Letters 18, 200 (1965).
3. M. A. Wahlig and I. Mannelli, Phys. Rev. 168, 1515 (1968).
4. V. N. Bolotov et al., Nuclear Physics B73, 387 (1974).

5. At 20 GeV the upstream beam hodoscope was removed in order to minimize multiple scattering, and the Cerenkov counter was used to eliminate electrons rather than to tag pions.
6. The detector will be described elsewhere in greater detail: A. V. Barnes, A. V. Tollestrup and R. L. Walker, manuscript in preparation.
7. The moments algorithms were developed in 1970-71 while planning the experiment. They are described in the reports listed under reference 1 of the preceding Letter on charge exchange scattering[1].

Captions

Table 1. Differential cross sections in $\mu b/GeV^2$ and other results for $\pi^- p \to \eta n$, $\eta \to 2\gamma$. These data have been corrected for the effects of instrumental t-resolution and finite bin widths. Only statistical errors and errors in t-dependent corrections are given for $\frac{d\sigma}{dt}$ but all systematic errors are included in the integral cross sections σ_I. The right-hand column, $\alpha^*(t)$, contains values of the trajectory obtained by fitting the data at each value of t separately.

Figure 1. (a) Schematic arrangement of the experimental apparatus (not to scale). The distance between hydrogen target and detector was scaled with energy: L = (16 m)(E/100 GeV). The location and window openings of V_2, V_3 and V_4 were adjusted accordingly. (b) The detector.

Figure 2. Mass histogram for two-photon events from the 64.4 GeV data. The events comprising this histogram have passed all cuts used to define charge exchange scattering or the $\pi^- p \to \eta n$ reaction with the exception of the mass cuts.

Figure 3. Differential cross sections for the reaction $\pi^- p \to \eta n$ with $\eta \to 2\gamma$ at 20.8, 64.4 and 199.3 GeV from this experiment and at 5.9 GeV from the experiment of reference 2. The curves are the result of a fit described in the text.

Figure 4. The effective trajectory $\alpha(t)$.

$-t$ (GeV^2)	Bin Width (GeV^2)	Beam Momentum in GeV						$\alpha^*(t)$
		20.8	40.8	64.4	100.7	150.2	199.3	
0.004	0.008	8.3 ± 1.0	3.14 ± 0.36	1.65 ± 0.20	0.98 ± 0.12	0.63 ± 0.08	0.46 ± 0.06	0.364 ± 0.036
0.012	0.008	8.5 ± 1.0	4.94 ± 0.46	1.82 ± 0.22	1.15 ± 0.14	0.74 ± 0.09	0.42 ± 0.06	0.333 ± 0.031
0.020	0.008	11.1 ± 1.2	3.87 ± 0.41	1.93 ± 0.23	1.41 ± 0.15	0.60 ± 0.08	0.69 ± 0.08	0.343 ± 0.034
0.032	0.016	10.2 ± 0.8	4.19 ± 0.31	2.24 ± 0.17	1.09 ± 0.09	0.84 ± 0.07	0.57 ± 0.05	0.355 ± 0.023
0.050	0.020	12.1 ± 0.8	4.52 ± 0.28	2.40 ± 0.16	1.31 ± 0.09	0.82 ± 0.06	0.55 ± 0.04	0.319 ± 0.019
0.070	0.020	11.0 ± 0.7	4.73 ± 0.28	2.56 ± 0.17	1.41 ± 0.09	0.82 ± 0.06	0.54 ± 0.04	0.335 ± 0.018
0.090	0.020	12.8 ± 0.8	4.70 ± 0.28	2.22 ± 0.16	1.42 ± 0.09	0.89 ± 0.06	0.56 ± 0.04	0.320 ± 0.019
0.110	0.020	12.3 ± 0.8	4.80 ± 0.29	2.09 ± 0.15	1.18 ± 0.09	0.61 ± 0.05	0.50 ± 0.04	0.261 ± 0.020
0.140	0.040	11.0 ± 0.5	4.22 ± 0.20	2.10 ± 0.11	1.08 ± 0.06	0.65 ± 0.04	0.447 ± 0.028	0.285 ± 0.015
0.180	0.040	9.9 ± 0.5	3.76 ± 0.18	1.68 ± 0.10	0.94 ± 0.06	0.423 ± 0.030	0.331 ± 0.024	0.226 ± 0.016
0.220	0.040	8.5 ± 0.5	2.99 ± 0.17	1.48 ± 0.09	0.73 ± 0.05	0.357 ± 0.028	0.229 ± 0.020	0.204 ± 0.017
0.260	0.040	7.4 ± 0.4	2.30 ± 0.14	1.15 ± 0.08	0.54 ± 0.04	0.236 ± 0.023	0.153 ± 0.016	0.147 ± 0.020
0.310	0.060	5.56 ± 0.32	1.84 ± 0.11	0.78 ± 0.06	0.344 ± 0.027	0.170 ± 0.016	0.091 ± 0.010	0.105 ± 0.019
0.370	0.060	3.91 ± 0.26	0.97 ± 0.07	0.47 ± 0.04	0.208 ± 0.021	0.105 ± 0.012	0.065 ± 0.009	0.094 ± 0.026
0.450	0.100	2.23 ± 0.15	0.64 ± 0.05	0.279 ± 0.025	0.109 ± 0.012	0.052 ± 0.007	0.024 ± 0.004	0.033 ± 0.025
0.550	0.100	1.16 ± 0.11	0.27 ± 0.03	0.117 ± 0.016	0.046 ± 0.008	0.0166 ± 0.0038	0.0100 ± 0.0028	-0.042 ± 0.039
0.700	0.200	0.47 ± 0.05	0.093 ± 0.013	0.033 ± 0.006	0.0134 ± 0.0031	0.0037 ± 0.0014	0.0020 ± 0.0009	-0.178 ± 0.053
0.900	0.200	0.102 ± 0.023	0.019 ± 0.006	0.006 ± 0.003	0.0034 ± 0.0016	0.0016 ± 0.0009	0.0012 ± 0.0007	-0.068 ± 0.128
1.100	0.200	0.031 ± 0.012	0.011 ± 0.004	0.0027 ± 0.0018	0.0015 ± 0.0010	0.0012 ± 0.0008	0.0002 ± 0.0003	-0.012 ± 0.156
$\frac{d\sigma}{dt}(t=0)$ from fit		6.71	2.88	1.62	0.92	0.558	0.391	
$\sigma_I(\mu b)=\int_{-1.5}^{0}\frac{d\sigma}{dt}\,dt$		3.85 ± 0.24	1.36 ± 0.09	0.647 ± 0.044	0.337 ± 0.021	0.184 ± 0.012	0.125 ± 0.008	
Number of events		4500	5100	3500	3300	2500	2100	

Table 1

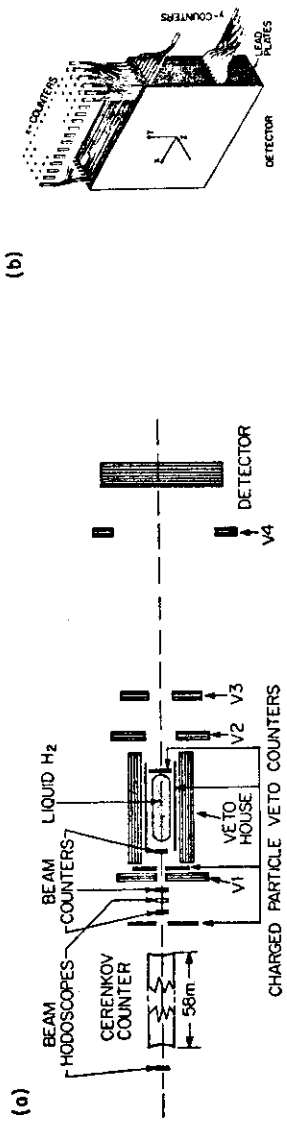
(a)
BEAM HODOSCOPES
CERENKOV COUNTER
58m
BEAM COUNTERS
LIQUID H_2
V1
V2
V3
V4
VETO HOUSE
CHARGED PARTICLE VETO COUNTERS
DETECTOR
(b)
γ-COUNTERS
γ-COUNTERS
LEAD PLATES
DETECTOR

Fig. 1

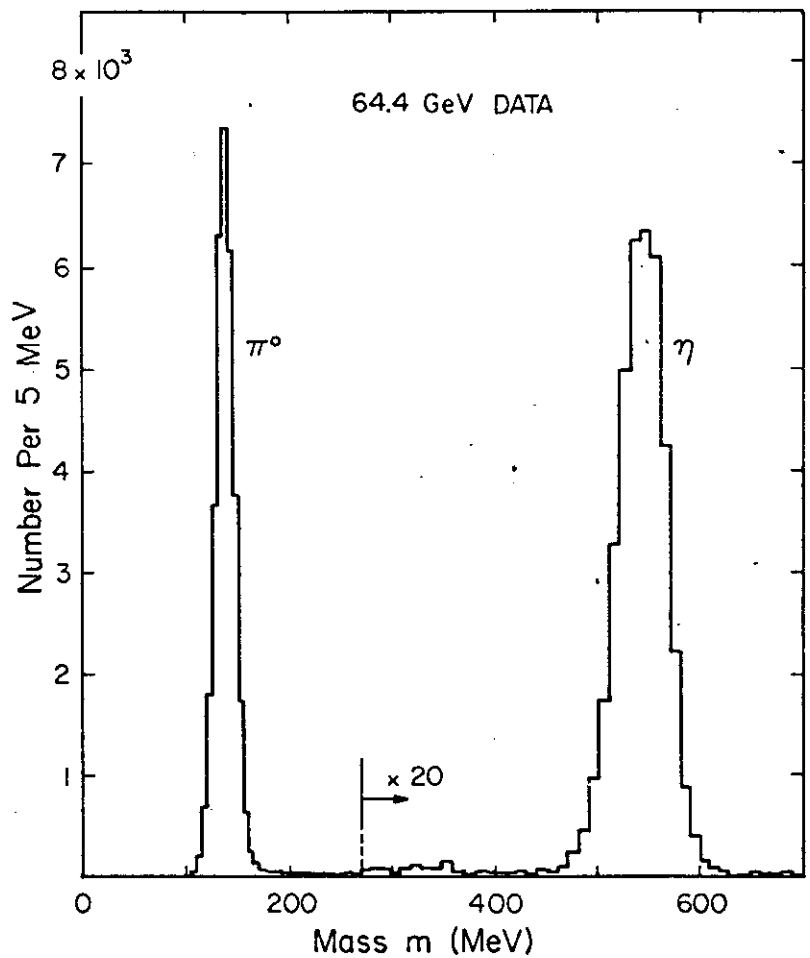
64.4 GeV DATA
8×10^3
7
6
5
4
3
2
1
Number Per 5 MeV
π^0
η
× 20
0
200
400
600
Mass m (MeV)

Fig. 2

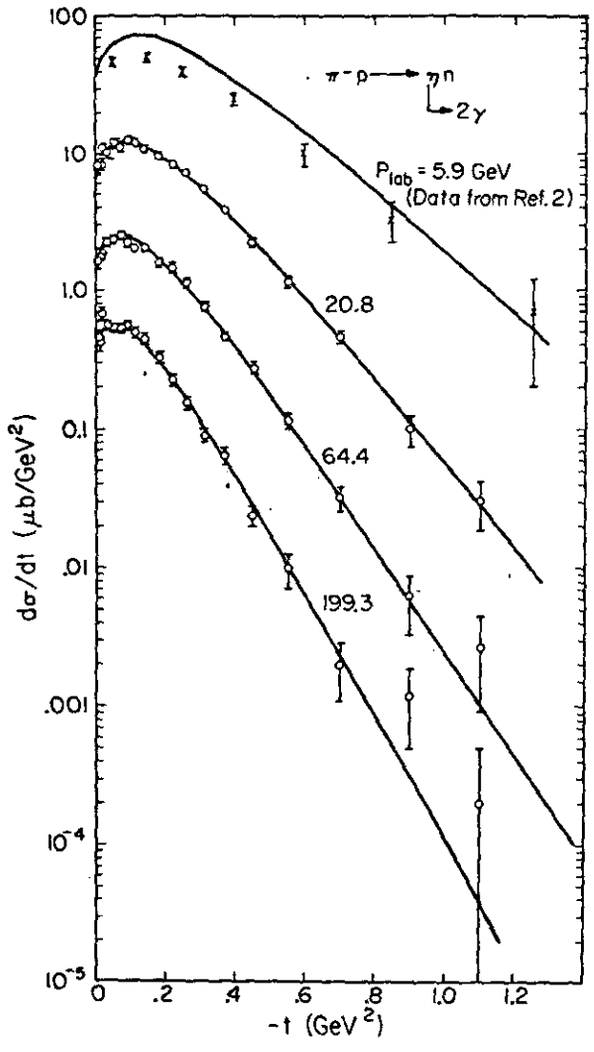
$\pi^- p \to \eta n$
$\to 2\gamma$
P_{lab} = 5.9 GeV
(Data from Ref. 2)
20.8
64.4
199.3
$d\sigma/dt$ (μb/GeV^2)
-t (GeV^2)

Fig. 3

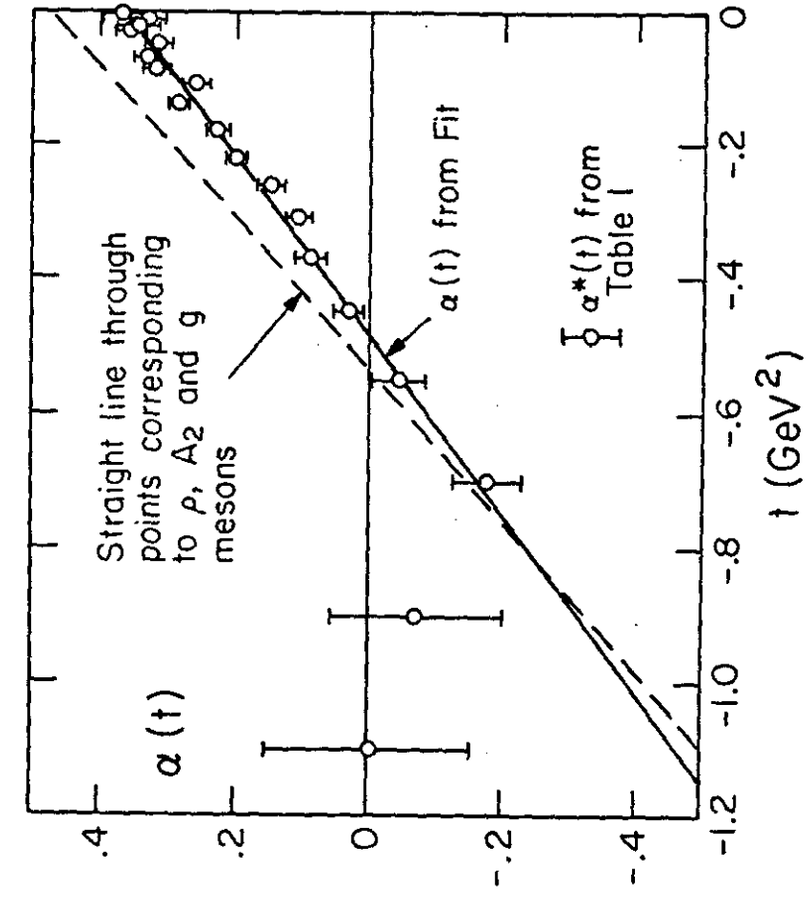
Straight line through points corresponding to ρ, A_2 and g mesons
$\alpha(t)$ from Fit
$\alpha^*(t)$ from Table I
$\alpha(t)$
t (GeV^2)

Fig. 4